nature biotechnology

Integration of chemical-genetic and genetic interaction data links bioactive compounds to cellular target pathways

Ainslie B Parsons[1,2], Renée L Brost[2], Huiming Ding[2], Zhijian Li[1,2], Chaoying Zhang[3], Bilal Sheikh[2], Grant W Brown[3], Patricia M Kane[4], Timothy R Hughes[1,2] & Charles Boone[1,2]

Bioactive compounds can be valuable research tools and drug leads, but it is often difficult to identify their mechanism of action or cellular target. Here we investigate the potential for integration of chemical-genetic and genetic interaction data to reveal information about the pathways and targets of inhibitory compounds. Taking advantage of the existing complete set of yeast haploid deletion mutants, we generated drug-hypersensitivity (chemical-genetic) profiles for 12 compounds. In addition to a set of compound-specific interactions, the chemical-genetic profiles identified a large group of genes required for multidrug resistance. In particular, yeast mutants lacking a functional vacuolar H^+-ATPase show multidrug sensitivity, a phenomenon that may be conserved in mammalian cells. By filtering chemical-genetic profiles for the multidrug-resistant genes and then clustering the compound-specific profiles with a compendium of large-scale genetic interaction profiles, we were able to identify target pathways or proteins. This method thus provides a powerful means for inferring mechanism of action.

For the yeast *Saccharomyces cerevisiae*, each of the ~6,000 potential genes characterized by the genome sequencing project has been deleted, identifying ~1,000 essential genes and ~5,000 viable deletion mutants[1]. Testing the viable mutants for hypersensitivity to a target-specific compound identifies a chemical-genetic interaction profile, which, for highly specific compounds, consists of a set of genes that buffer the cell from defects in target activity (**Fig. 1a**). Because a loss-of-function mutation in a gene encoding the target of an inhibitory compound models the primary effect of the compound[2–4], crossing such a mutation into the set of viable mutants and scoring the resultant double mutants for reduced fitness should generate a genetic interaction profile for the target gene that resembles the chemical-genetic interaction profile of its inhibitory compound (**Fig. 1b**). We therefore expected that a comprehensive compendium of global genetic interaction profiles would provide a key for deciphering the pathways and targets of growth-inhibitory compounds. To establish this proof of concept, we applied a four-step strategy to link several well-characterized compounds to their target pathways and proteins.

1. We screened 12 inhibitory compounds against the *S. cerevisiae* viable deletion set to generate chemical-genetic interaction profiles.
2. We identified sets of genes that occur in multiple chemical-genetic interaction profiles and thus may contribute to general multidrug resistance. Filtering the multidrug-resistant genes from the chemical-genetic interaction profiles enabled us to generate compound-specific profiles.
3. We generated genetic interaction profiles for genes encoding compound targets by conducting synthetic genetic array (SGA) analysis[5] with query mutations in target genes.
4. We carried out clustering analysis of chemical-genetic profiles with a compendium of genetic interaction profiles and thereby grouped several compounds with their known target pathways or proteins.

RESULTS

Generation of chemical-genetic interaction profiles

We screened ~4,700 viable yeast deletion mutants for hypersensitivity to 12 diverse inhibitory compounds (see **Supplementary Tables 1** and **2** online). These compounds included benomyl, a microtubule depolymerizing agent[6]; FK506 and cyclosporin A (CsA), immunosuppressant drugs that inhibit calcineurin[7]; hydroxyurea, an inhibitor of ribonucleotide reductase[8]; camptothecin, a topoisomerase I inhibitor[9]; fluconazole, an antifungal drug that inhibits Erg11, a cytochrome P450 required for ergosterol biosynthesis[10,11]; cycloheximide, an inhibitor of protein synthesis; rapamycin, an inhibitor of TOR kinase signaling[12]; tunicamycin, an inhibitor of protein glycosylation[13]; wortmannin, an inhibitor of phosphatidylinositol kinase signaling[14]; sulfometuron methyl, an inhibitor of amino acid biosynthesis[15]; and caffeine, an inhibitor of cAMP phosphodiesterases[16]. The

[1]Department of Molecular and Medical Genetics, [2]Banting and Best Department of Medical Research, and [3]Department of Biochemistry, University of Toronto, Toronto, Ontario M5G 1L6, Canada. [4]Department of Biochemistry, State University of New York, Upstate Medical University, Syracuse, New York 13210, USA. Correspondence should be addressed to C.B. (charlie.boone@utoronto.ca).

Published online 7 December 2003; doi:10.1038/nbt919

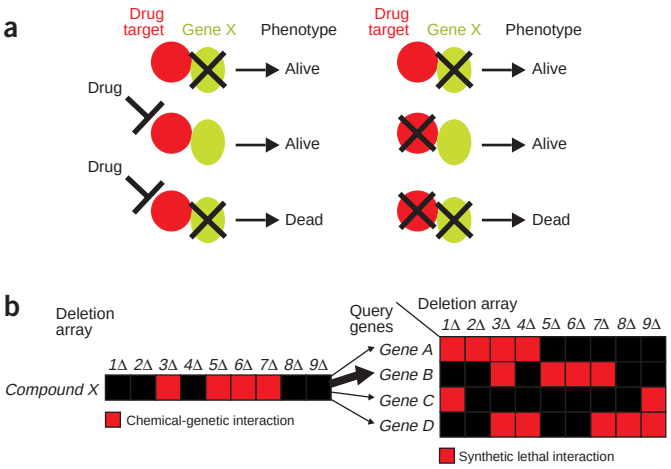

Figure 1 Chemical-genetic interactions can be modeled by synthetic genetic interactions. (**a**) In a chemical-genetic interaction (at left), a deletion mutant, lacking the product of the deleted gene (represented by a black X), is hypersensitive to a normally sublethal concentration of a growth-inhibitory compound. In a synthetic lethal genetic interaction (right), two single deletions lead to viable mutants but are inviable in a double -mutant combination. Gene deletion alleles that show chemical-genetic interactions with a particular compound should also be synthetically lethal or sick with a mutation in the compound target gene. (**b**) Comparison of a chemical-genetic profile to a compendium of genetic interaction (synthetic lethal) profiles should identify the pathways and targets inhibited by drug treatment. In this hypothetical figure, chemical-genetic and genetic interactions are both designated by red squares. For example, deletion mutants *3*Δ, *5*Δ, *6*Δ and *7*Δ are hypersensitive to compound X and a mutation in query *gene A* leads to a fitness defect when combined with deletion alleles *1*Δ, *2*Δ, *3*Δ and *4*Δ. Here, the chemical-genetic profile of compound X resembles the genetic profile of *gene B*, thereby identifying the product of *gene B* as a putative target of compound X.

hypersensitive mutants were identified by arraying strains onto agar plates containing semi-inhibitory concentrations of each compound and scoring reduced colony formation. These putative chemical-genetic interactions were then confirmed by serial-dilution spot assays in a second round of analysis, such that the final data set should contain few false positives.

To address potential false negatives, we compared the results from our rapamycin screen to those published previously (see **Supplementary Table 3** online). Our deletion mutant array contains 85 strains characterized previously as rapamycin sensitive, 39 of which we identified within our total set of 246 rapamycin-sensitive strains. Of the remaining 46 published interactions, we were able to confirm 22 strains as

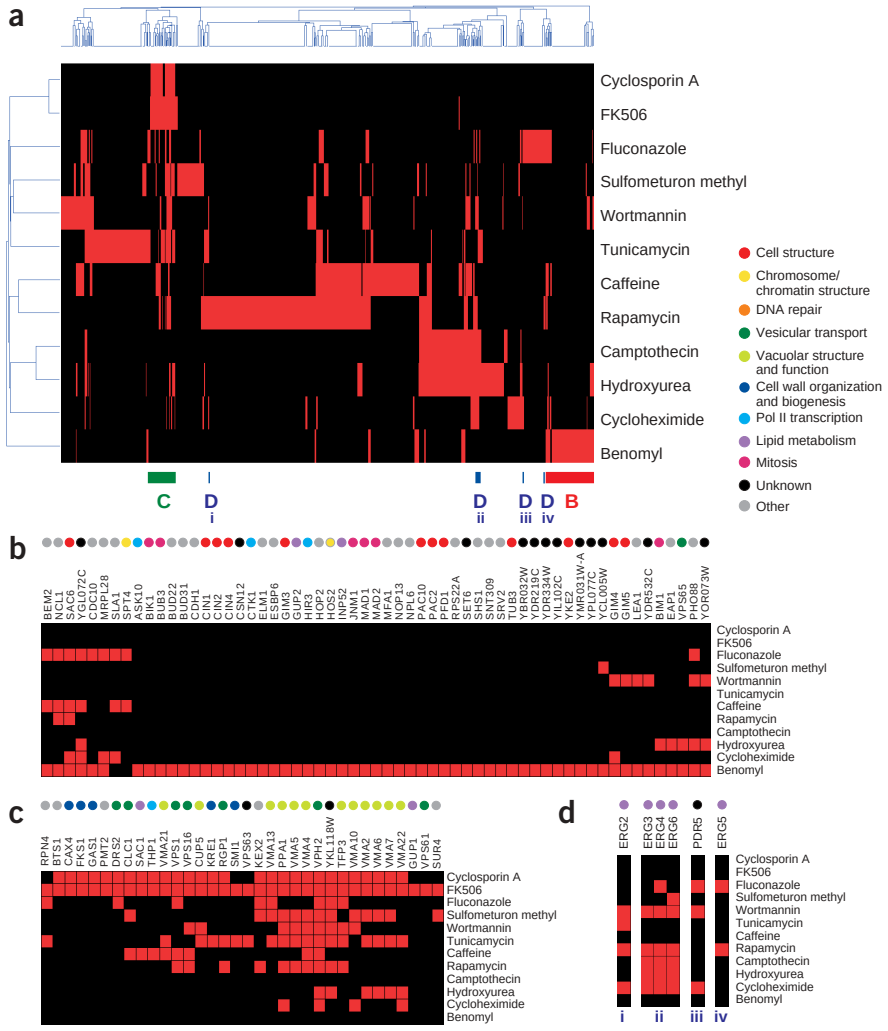

Figure 2 The set of viable gene deletion mutants were screened for hypersensitivity to each of 12 inhibitory compounds (cyclosporin A, FK506, tunicamycin, sulfometuron methyl, wortmannin, caffeine, rapamycin, fluconazole, camptothecin, hydroxyurea, cycloheximide and benomyl). (**a**) Two-dimensional hierarchical cluster plot of chemical-genetic profiles. Genes are represented on the horizontal axis and compounds on the vertical axis, with chemical-genetic interactions shown in red. Both compounds and genes are clustered together based upon the similarity of their chemical-genetic interactions. (**b**) A section of the cluster plot (red bar, labeled 'B' on the horizontal axis of **a**) is enlarged to highlight gene deletions that lead to benomyl sensitivity specifically. Genes involved in tubulin folding (*CIN1*, *CIN2*, *CIN4*), the prefoldin actin/tubulin chaperone complex (*GIM3, GIM4, GIM5, PAC2, PAC10, PFD1, YKE2*), the mitotic spindle checkpoint (*MAD1, MAD2, BUB3*) and tubulin structure (*TUB3*) showed chemical-genetic interactions with benomyl. (**c**) A section of the cluster plot (green bar, labeled 'C' on the horizontal axis of **a**) is enlarged to show the overlap between the CsA and FK506 chemical-genetic interaction profiles. (**d**) Several different sections of the cluster plot (blue bars, labeled 'D i', 'D ii', 'D iii', 'D iv' on the horizontal axis of **a**) are enlarged to show the multidrug sensitivity associated with gene deletions in *ERG2*, *ERG3*, *ERG4*, *ERG5*, *ERG6* and *PDR5*.

slightly or moderately sensitive to rapamycin by spot assay. For the remaining 24 strains, we did not detect any sensitivity, which may reflect differences associated with the sensitivity assays or false positives in the published data. Thus, our screening system offers broad coverage and readily identifies strains that are strongly sensitive to inhibitory compounds; however, we may miss a number of strains with partial sensitivity.

To visualize the entire set of chemical-genetic interactions, we analyzed the profiles by two-dimensional hierarchical clustering (**Fig. 2a**). The plot shows 12 chemical screens that interacted with 647 different genes. Compounds with similar chemical-genetic interaction profiles were clustered on the vertical axis and the genes associated with similar patterns of compound sensitivities were clustered on the horizontal axis. For example, the profile of benomyl, a microtubule depolymerizing agent, was unique because it was the only compound we examined with interactions enriched for genes involved in cell structure, chromosome structure and mitosis (**Fig. 2b**). In contrast, the calcineurin inhibitors CsA and FK506 cluster together on the vertical axis because they have highly similar chemical-genetic interaction profiles. Their profiles are enriched for genes involved in cell wall organization and vacuolar structure and function (**Fig. 2c**), reflecting the established role of calcineurin in cell wall homeostasis and vacuolar function[17].

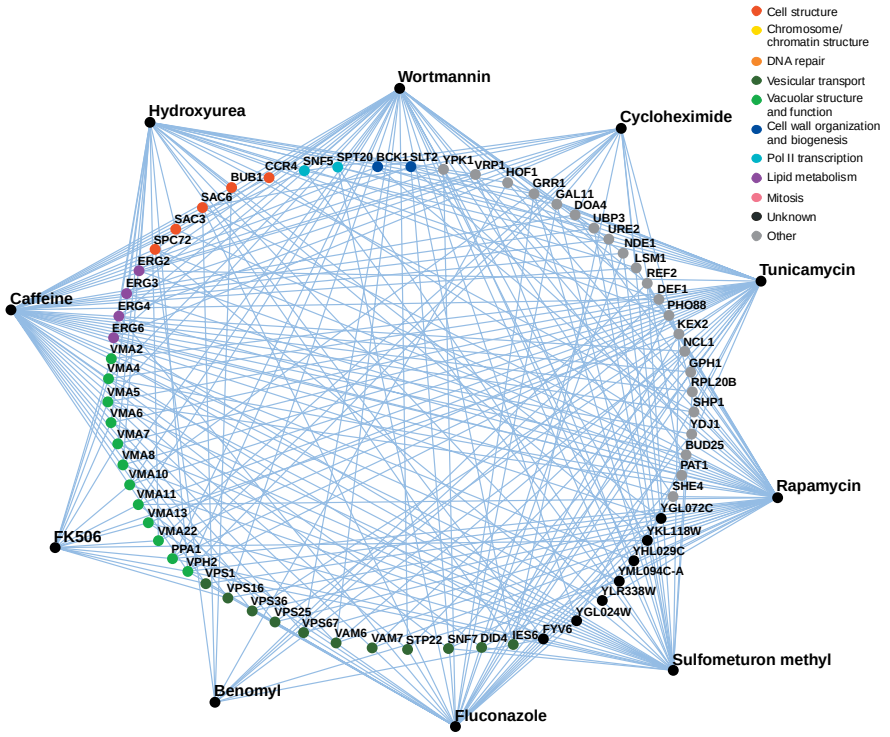

Figure 3 To classify multidrug resistance genes, we identified 65 deletion strains that were sensitive to at least four of ten diverse compounds: wortmannin, benomyl, tunicamycin, rapamycin, sulfometuron methyl, fluconazole, cycloheximide, FK506, caffeine and hydroxyurea. The camptothecin chemical-genetic profile was excluded from this analysis because it overlaps extensively with the hydroxyurea profile and the CsA profile was excluded because it overlaps extensively with that of FK506. In the network diagram, edges indicate a chemical-genetic interaction and nodes represent either compounds or genes, with the genes color-coded from a defined subset of GO functional attributes.

Identification of a multidrug-resistant gene set

The hierarchical clustering revealed a number of genes associated with sensitivity to multiple compounds with diverse modes of action. Drug efflux pumps and members of the ATP-binding cassette protein family, such as Pdr5, Yor1 and Snq1, protect yeast from a range of drugs and confer multidrug resistance when overexpressed[18]. Membrane lipid composition also affects drug susceptibility in yeast, as deletion mutants defective for ergosterol biosynthesis have high membrane fluidity and show hypersensitivity to numerous drugs[19]. Indeed, we found that *pdr5*Δ cells were hypersensitive to cycloheximide, fluconazole and wortmannin and that cells deleted for genes encoding ergosterol biosynthetic enzymes such as *ERG3*, *ERG4* and *ERG6* were sensitive to wortmannin, rapamycin, camptothecin, hydroxyurea and cycloheximide (**Fig. 2d**). We also identified a number of new strains as multidrug sensitive (see, for example, *VPH2* in **Fig. 2c**). To define a multidrug-resistant gene set, we constructed a chemical-genetic interaction network of the 65 genes associated with sensitivity to four or more compounds (**Fig. 3**). This network was enriched for genes involved in vacuolar protein sorting (*VPS16, VPS25, VPS36, VPS67, VAM7, VAM6, STP22, SNF7, DID4, IES6*) and genes encoding subunits of the yeast vacuolar H^+-ATPase complex (*VMA2, VMA4, VMA5, VMA6, VMA7, VMA8, VMA10, VMA13, VMA22, PPA1, VMA11, VPH2*), a proton pump that maintains the low vacuolar pH (gene data obtained from the Saccharomyces Genome Database, www.yeastgenome.org). These findings are consistent with previous observations identifying *vma* and *vps* mutants as sensitive to staurosporine, vanadate and hygromycin B[20].

Some of the highly conserved genes in the yeast multidrug-resistant gene set may also control drug resistance in mammalian cells. Indeed, three lines of evidence suggest that the role of the vacuolar H^+-ATPase in multidrug resistance may be conserved. First, in mammalian cell culture, changes in intracellular pH can alter drug accumulation[21]. Second, the gene encoding vacuolar H^+-ATPase subunit C is overexpressed in multidrug-resistant HL60 cells[22], and exposure to concanamycin A, an inhibitor of vacuolar H^+-ATPases[23], can restore the sensitivity of drug-resistant cells to several anticancer drugs, including daunomycin, doxorubicin and epirubicin[24]. Third, we found that the effect of the actin depolymerizing agent latrunculin A on mammalian cells was enhanced by inhibition of the vacuolar H^+-ATPase with concanamycin A (see **Supplementary Figs. 1** and **2** and **Supplementary Methods** online).

Generation of genetic interaction profiles for compound targets

To compare chemical-genetic interaction profiles with genetic interaction data derived from genes encoding compound targets, we first performed SGA analysis with a query mutation in *ERG11*, which encodes the target of the antifungal drug fluconazole. Because *ERG11* is an essential gene, we created a temperature-sensitive query mutation using the heat-induced degron system[25] and then screened for synthetic genetic interactions at a permissive temperature. SGA analysis enables a query mutation to be crossed into the set of viable deletion mutants such that the resultant double mutants can be screened for synthetic lethal or sick (slow-growing) interactions[5]. **Figure 4** shows a comparison of the fluconazole chemical-genetic interactions and the

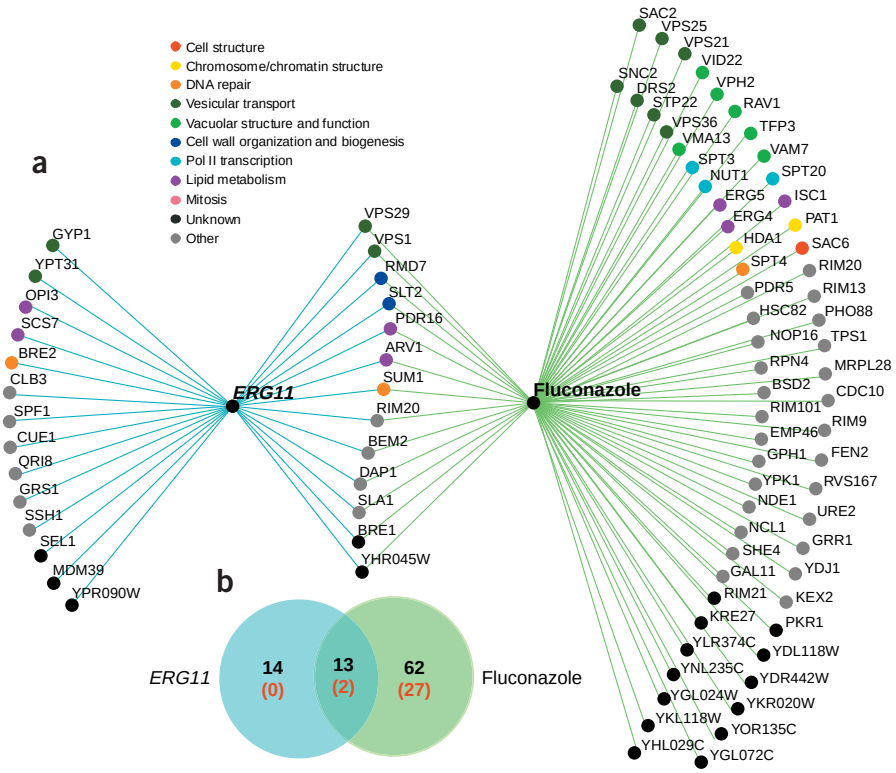

Figure 4 Overlap between the chemical-genetic profile of fluconazole and the genetic interaction profile of *ERG11*. Edges indicate either a chemical-genetic or a genetic interaction and nodes represent either compounds or genes, with the gene nodes color-coded from a defined subset of GO functional attributes. (**a**) Network of the chemical-genetic interactions with fluconazole and the genetic interactions with *ERG11*. (**b**) Venn diagram summarizing that 75 genes showed a chemical-genetic interaction with fluconazole, 27 genes showed a genetic interaction with *ERG11* and 13 genes were in the overlap set. Red bracketed numbers indicate the number of genes, in each group, classified as multidrug resistant.

ERG11 genetic interactions. In total, 27 genes were identified as synthetic lethal or sick with *ERG11*, of which 13 were also fluconazole sensitive. Genes involved in lipid metabolism (*PDR16, ARV1*), cell wall organization and morphogenesis (*RMD7, SLT2*) and uncharacterized function (*YHR045W*) were identified in both the genetic and chemical-genetic screens (**Fig. 4a**, **Supplementary Table 4** online).

We next examined calcineurin, a highly conserved protein phosphatase required in yeast under a number of environmental conditions such as ionic stress, high pH and exposure to prolonged mating pheromone[26]. Calcineurin can be inactivated genetically, by deletion of *CNB1*, which encodes its regulatory subunit[27], or chemically, by treatment with the immunosuppressant drugs FK506 or CsA[7]. From SGA analysis with a *cnb1*Δ query mutation, we identified 3 of the 4 nonessential genes known to be synthetically lethal with *CNB1* (refs. 17,28; *FKS1, CUP5, VPH2*) and identified 35 new synthetic genetic interactions (see **Supplementary Table 4** online). Comparison of the *CNB1* synthetic genetic interactions with the FK506 and CsA chemical-genetic interactions showed that they largely overlap (**Fig. 5a**). Of the 38 genes that interacted genetically with *CNB1*, 23 were hypersensitive to both FK506 and CsA and a further 5 were hypersensitive to FK506 alone.

For all three drugs, the overlap between the chemical-genetic and genetic interaction profiles was found to be highly significant when compared to random data sets. For example, it is highly unlikely that one would obtain the observed overlap between the genetic profile of *ERG11* and the chemical profile of fluconazole by chance ($P = 3.8 \times 10^{-56}$). Discrepancy between the chemical-genetic and genetic profiles of compounds and their targets could be a result of incomplete inactivation of the target protein function by the drugs or may reflect the inherent differences in genetic versus chemical mechanisms of target inhibition; unlike a gene deletion that eliminates the target protein from the cell, chemical inhibitors form a complex with the target proteins and the inactive complex remains physically present. In particular, genes that show a chemical-genetic interaction with a drug but not a genetic interaction with the drug target could be involved in cellular import or export of compounds or may provide insight into drug off-target effects.

Twenty-nine genes found in the fluconazole profile were members of the multidrug-resistant gene set (**Fig. 4b**, red bracketed numbers) and removal of these interactions increased the overlap with the *ERG11* genetic interaction profile. In the case of the FK506 and CsA profiles, 15 genes were members of multidrug-resistant gene set; however, 12 of these also showed a genetic interaction with *CNB1* (**Fig. 5b**), including nine vacuolar H^+-ATPase (*vma*) mutants, which reflects an established synthetic lethal relationship[17,28]. Because *vma* mutants do not seem to be identified commonly in SGA screens (ref 5 and A.H.Y. Tong, G. Lesage, G. Bader, H.D., H. Xu, X. Xin *et al.*, unpublished data), this may be a rare example where the chemical-genetic interactions observed for genes within the multidrug-resistant gene set actually reflect a target gene specificity. Nevertheless, even with the 12 multidrug-resistant genes removed from the FK506 and CsA profiles, the overlaps with the *CNB1* genetic interaction profile remain highly significant ($P = 4.4 \times 10^{-53}$ and $P = 2.7 \times 10^{-60}$, respectively).

Clustering of chemical-genetic and genetic interaction profiles

To assess whether a comparison of chemical-genetic to genetic interaction profiles can be used to identify the target pathways of inhibitory compounds, we performed two-dimensional hierarchical clustering of a combined data set. We focused on the chemical-genetic screens for FK506, CsA, fluconazole, benomyl, hydroxyurea and camptothecin, and we collected genetic interaction data either for the gene encoding the drug target or for functionally related genes whose products function within the pathway affected by the compound. These chemical-genetic screens were compared to a compendium of 57 genetic interaction screens, derived from query genes with roles in DNA synthesis and repair, secretion, cell wall biosynthesis, actin assembly, polarized morphogenesis, and microtubule structure and function (ref. 5 and A.H.Y. Tong, G. Lesage, G. Bader, H.D., H. Xu, X. Xin *et al.*, unpublished data). To identify specific chemical-genetic interactions, we first filtered the multidrug-resistance genes from the chemical-genetic profiles. In the resultant plot (**Fig. 6a**), the profiles associated with compounds and query genes are clustered on the vertical axis and those of

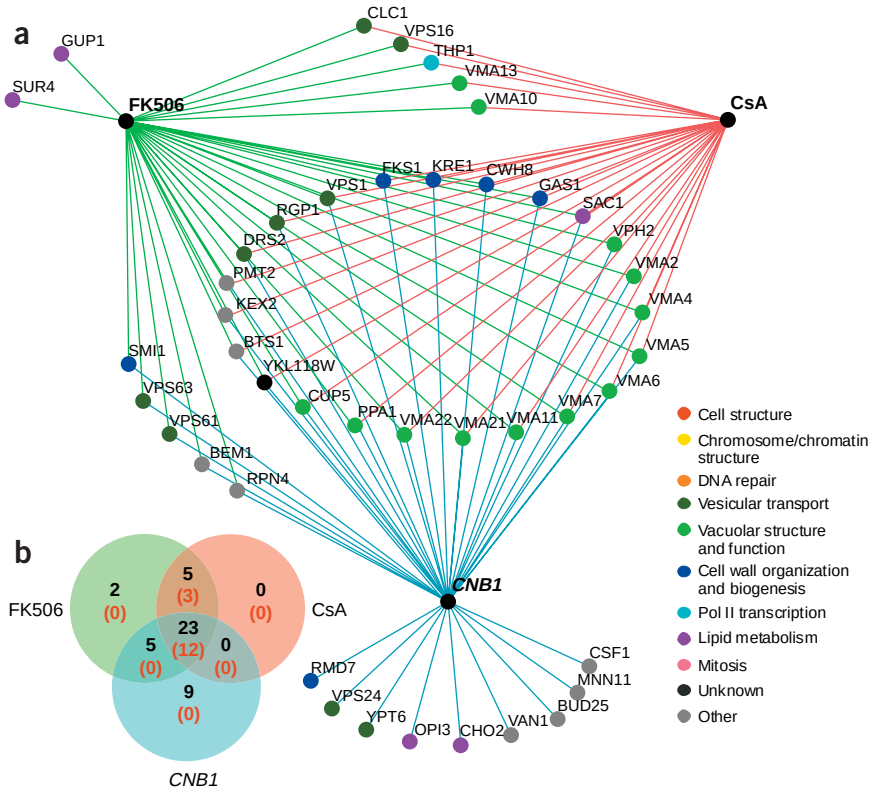

Figure 5 Overlap between the chemical-genetic profiles of FK506 and CsA and the genetic interaction profile of *CNB1*. Edges indicate either a chemical-genetic or a genetic interaction and nodes represent either compounds or genes, with the gene nodes color-coded from a defined subset of GO functional attributes. (**a**) Network of the chemical-genetic interactions of FK506 and CsA and the genetic interactions with *CNB1*. (**b**) Venn diagram summarizing that 35 genes showed a chemical-genetic interaction with FK506, 28 genes showed a chemical genetic interaction with CsA and 38 genes showed a genetic interaction with *CNB1*, with 24 interactions common to all three screens. Red bracketed numbers indicate the number of genes, in each group, classified as multidrug resistant.

the 803 interacting genes are clustered on the horizontal axis. The genetic interaction profile of *ERG11* clustered with the chemical-genetic profile of fluconazole and the genetic interaction profile of *CNB1* clustered with the chemical-genetic profiles of FK506 and CsA. Similarly, the chemical-genetic interaction profile for benomyl clustered with *TUB2* and other genes encoding proteins with roles in microtubule structure and function, such as *GIM3*, a component of the prefoldin complex involved in tubulin folding; *CIN1*, a tubulin folding cofactor; *KAR3*, a minus end–directed kinesin; and *MAD2*, a spindle checkpoint protein. In the case of hydroxyurea and camptothecin, the chemical-genetic profile clustered with genes whose products have roles in DNA synthesis, such as *POL32*, a subunit of DNA polymerase delta, and *RAD27*, a 5′-to-3′ exonuclease required for Okazaki fragment processing, linking these compounds with the cellular function they inhibit, even though the actual target genes were not represented in the cluster. Thus, a compendium of genetic interaction profiles provides a key for interpreting chemical-genetic interaction profiles and can link compounds to their cellular pathways and/or targets.

Overlapping chemical and genetic datasets can provide corroborative evidence to implicate uncharacterized genes in specific roles (**Fig. 6b**). For example, the uncharacterized open reading frame (ORF) *VID21* was identified as sensitive to camptothecin and hydroxyurea and showed a genetic interaction with *POL32*. Domain analysis of the Vid21 sequence revealed a SANT domain and the SANT-associated helicase domain HSA. The SANT domain was first identified based on its homology to the DNA binding domain of c-Myb[29] but is a common domain found in chromatin remodeling enzymes[30], indicating a possible role for Vid21 in chromatin remodeling after DNA damage. Additionally, the uncharacterized ORF *YBR094W* was identified as highly sensitive to both camptothecin and hydroxyurea and also interacts genetically with *CDC2*, which encodes a subunit of DNA polymerase III; *ELG1*, whose product forms an alternative replication factor C (RFC) complex important for DNA replication[31,32]; *ESC2*, a gene involved in establishing silent chromatin; and *SGS1*, which encodes a DNA helicase involved in DNA replication and maintenance of genome stability. The *YBR094W* product contains a tubulin tyrosine ligase domain[33], suggesting that it may encode an enzyme responsible for post-translational modification of proteins involved in the DNA damage response.

DISCUSSION

Taken together, these results demonstrate the potential for integration of chemical-genetic profiles and genetic interaction profiles to provide information about the pathways and targets affected by bioactive compounds. A chemical-genetic profile can be generated for any compound that is inhibitory to the growth of wild-type yeast or a subset of the deletion mutants. As the compendium of yeast genetic interaction profiles grows and ultimately covers most cellular pathways, it will become a more powerful tool for assessing compound function. From large-scale mapping of genetic interactions with the set of deletion mutants, we find that clustering genes showing similar patterns of genetic interactions identifies pathway components but often does not distinguish their order within the pathway (ref. 5 and A.H.Y. Tong, G. Lesage, G. Bader, H.D., H. Xu, X. Xin *et al.*, unpublished data). Consequently, direct application of this approach may link compounds to a target pathway, but identification of the precise target would be likely to require specific analysis of the pathway components. To screen compounds that are in limited supply, parallel fitness tests with pooled deletion mutants and a microarray readout[1,34] could be used to generate chemical-genetic profiles. Indeed, results similar to those detailed here were obtained by this method (data not shown). Mutations in genes encoding the multidrug-resistant gene set or compounds that inhibit their targets, such as the vacuolar H^+-ATPase inhibitor concanamycin A, could be used to generate a sensitized assay. Chemical-genetic profiling complements other yeast genomic methodologies, such as gene expression profiling experiments[2,3] and chemically induced haploinsufficiency analysis[35], that also tackle the problem of linking drugs to their targets. The chemical-genetic screening described here offers some unique advantages over these methods. For example, it generates a rich set of functional information about the pathways normally required to buffer the effects of the compound. In this regard, chemical-genetic screening is also particularly valuable in cases where a compound does not inhibit

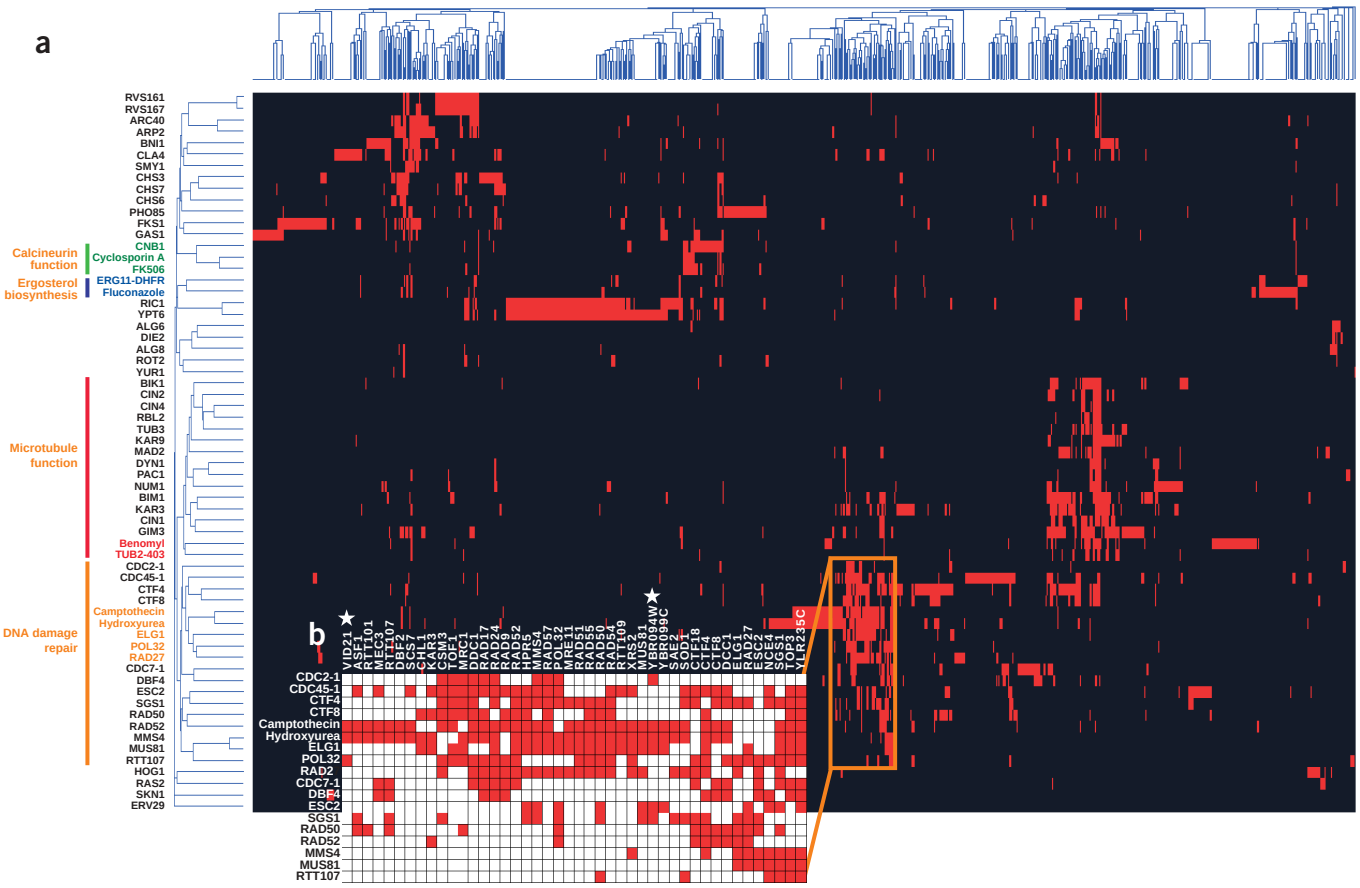

Figure 6 Two-dimensional hierarchical clustering analysis of chemical-genetic and genetic interaction profiles. (**a**) Six chemical-genetic profiles (FK506, CsA, fluconazole, benomyl, hydroxyurea and camptothecin) were clustered with 57 genetic interaction profiles. Chemical-genetic or genetic interactions are represented in red. Interacting genes are plotted on the horizontal axis, with the gene cluster tree above. Compounds and query genes are plotted on the vertical axis, with the cluster tree on the outermost left side of the plot. Compounds that cluster with their target genes and pathways are colored similarly. The vertical red bar indicates a set of query genes involved in microtubule-based functions. The vertical orange bar indicates a set of query genes involved in DNA synthesis and repair. Sources of genetic interaction data include this study (*CNB1, ERG11-DHFR, TUB2-403*); ref. 5 (*ARC40, ARP2, BNI1, BIM1, RAD27, SGS1*); and (A.H.Y. Tong, G. Lesage, G. Bader, H.D., H. Xu, X. Xin *et al.*, unpublished data) (*RVS161, RVS167, SMY1, CLA4, CHS3, CHS7, CHS6, YUR1, PHO85, FKS1, GAS1, RIC1, YPT6, ALG6, DIE2, ALG8, ROT2, BIK1, CIN4, RBL2, TUB3, CIN1, CIN2, MAD2, DYN1, PAC1, NUM1, KAR3, KAR9, GIM3, CTF4, CTF8, POL32, DBF4, CDC2-1, CDC45-1, ELG1, CDC7-1, MMS4, MUS81, RTT107, RAD50, RAD52, RAD24, HOG1, RAS2, SKN1, ERV29*). All genetic interaction data are available at http://biodata.mshri.on.ca/grid. (**b**) Overlap of the chemical-genetic screens of camptothecin and hydroxyurea and genetic interaction screens for the set of query genes involved in DNA synthesis and repair. A section of the cluster plot (orange box in **a**) is enlarged. *VID21* and *YBR094W* are marked with an asterisk to indicate that these previously uncharacterized genes were identified by both chemical-genetic and genetic screens.

a specific protein target because it will highlight the primary pathways and cellular functions affected by the drug treatment. Finally, the concept of modeling chemical-genetic profiles with global genetic interaction profiles should be readily applicable to higher organisms. For example, large-scale RNA-mediated interference, transposon-based mutagenesis or morpholino-modified antisense oligonucleotide approaches can be used to generate large collections of defined mutants in *Drosophila melanogaster*, *Caenorhabditis elegans*, zebrafish and mammalian cell lines[36,37] and should allow for similar studies to be carried out in these systems.

METHODS

Strains and media. Yeast deletion strains derived from **BY4741** (*MAT***a** *his3Δ1 leu2Δ0 met15Δ0 ura3Δ0*) and generated by the *S. cerevisiae* deletion consortium[1] were maintained in an ordered array on agar plates at a density of 768 strains (384 unique strains arrayed in duplicate) per plate and manipulated robotically with a colony arrayer (Bio-Rad)[5].

For the chemical-genetic screens, drugs were added from concentrated stocks to autoclaved rich (YPD; 2% peptone, 1% yeast extract, 2% glucose and 2% agar) or synthetic complete (SC; 0.67% yeast nitrogen base without amino acids, 0.2% amino acid add back, 2% glucose and 2% agar) medium cooled to ~50 °C. Most drugs were screened and confirmed by spot assays at the same concentration; some were confirmed at a lower concentration, as noted: FK506 (2 μg/ml in SC; gift of M. Cyert and purchased from AG Scientific), CsA (100 μg/ml in SC; AG Scientific), hydroxyurea (100 mM in YPD; Sigma), camptothecin (15 μg/ml in YPD; gift of S. Brill and purchased from AG Scientific), fluconazole (15 μg/ml in YPD; gift of J. Anderson), tunicamycin (5 μg/ml and 0.5 μg/ml in YPD; AG Scientific), wortmannin (1.3 μg/ml in YPD; AG Scientific), caffeine (0.15% in SC; Sigma), rapamycin (0.015 μg/ml and 0.01 μg/ml in YPD; AG Scientific), benomyl (15 μg/ml in YPD; Sigma); sulfometuron methyl (3 μg/ml in SC; Sigma) and cycloheximide (0.1 μg/ml in YPD; Sigma).

For the synthetic genetic (SGA) screening, we used as sporulation medium 2% agar, 1% potassium acetate, 0.1% yeast extract and 0.05% glucose, supplemented with uracil, histidine and leucine. Filter-sterilized solutions of

L-canavanine (50 mg/l; Sigma), G418 (200 mg/l; Invitrogen Life Technologies) and clonNAT (100 mg/l; Werner Bioagents) were added to cooled media where indicated. In cases where SC medium was supplemented with clonNAT or G418, the ammonium sulfate was replaced with monosodium glutamate and the medium termed SC/MSG (0.17% yeast nitrogen base without amino acids and ammonium sulfate, 0.1% monosodium glutamic acid, 0.2% amino acid add back, 2% glucose and 2% agar).

Chemical-genetic screens. Genome-wide chemical-genetic profiles were generated by robotically pinning arrayed yeast strains onto solid medium containing drug at a semi-inhibitory concentration (a concentration where wild-type yeast growth is slightly compromised as compared to the no-drug control). All plates were incubated at 30 °C. The sensitivity of each of the ~4,700 haploid deletion strains to a particular drug was assayed by comparing colony size on drug plates versus a no-drug control. Each chemical was screened against the complete array at least three times; each interaction that was identified at least twice by manual scoring or by computer-based scoring was confirmed using serial-dilution spot assays. For the spot assays, deletion strains were grown overnight to saturation at 30 °C in 130 µl of YPD or SC liquid in a 96-well plate. Using a multichannel pipettor, each culture was diluted by five serial 100-fold dilutions and 2 µl of each dilution was spotted onto medium containing drug and a no-drug control medium. Plates were incubated at 30 °C for 2–4 d and scored for drug sensitivity. Mutants inviable at all dilutions on drug plates as compared to a no-drug control were designated as strongly sensitive and given a score of 3, mutants viable at only the first one or two dilutions were designated as moderately sensitive and given a score of 2, and mutants that grew at all dilutions, but more slowly, were designated as mildly sensitive and given a score of 1. Approximately 50–80% of interactions identified as putatively sensitive from the array screens were subsequently confirmed with spot assays. For the FK506, CsA, fluconazole and benomyl screens, all deletion mutants identified as synthetic lethal or synthetic sick with the appropriate drug target were also tested for chemical sensitivity by spot assay. All deletion mutants sensitive to camptothecin were also tested for sensitivity to hydroxyurea and all deletion mutants sensitive to hydroxyurea were also tested for sensitivity to camptothecin.

SGA analysis. Genome-wide synthetic lethal screens were performed using synthetic genetic array (SGA) analysis as described previously[5]. The *MAT*α starting strains, *cnb1*Δ::*URA3 mfa1*Δ::*MFA1pr-HIS3 can1*Δ (Y3404), *erg11 DHFR-ts*::*natR can1*Δ::*MFA1pr-HIS3-MF*α*1pr-LEU2* (Y4830) and *tub2-403*::*URA3 can1*Δ::*MFA1pr-HIS3-MF*α*1pr-LEU2* (Y4499), were derived from wild-type strain BY4742 (ref. 38). For SGA analysis, first the ordered array of ~4,700 *MAT***a** XXXΔ::*kanR* strains, where XXXΔ::*kanR* designates one of the ~4,700 deletion alleles, was crossed to a starting strain; second, the resultant diploids were selected; third, the diploids were pinned onto sporulation medium to induce meiosis; fourth, *MAT***a** meiotic progeny were germinated specifically; fifth, *MAT***a** XXXΔ::*kanR* meiotic progeny were selected; and sixth, *MAT***a** double mutants were selected. Diploids were selected on SC –Ura–Lys plates or YPD plates supplemented with G418 and clonNAT for 1 d at 30 °C and then sporulated for 5 d at room temperature. In particular, to select for *MAT***a** *can1*Δ::*MFA1pr-HIS3*::*MF*α*1pr-LEU2* meiotic progeny, spores were germinated on SC –His–Arg medium supplemented with L-canavanine for 2 d at 30 °C and then transferred onto a fresh plate of the same medium for another day of growth at 30 °C. The *MAT***a** meiotic progeny were then transferred to SC/MSG –His–Arg supplemented with L-canavanine and G418 to select for *MAT***a** XXXΔ::*kanR* meiotic progeny. Finally, cells were transferred to either SC/MSG –His–Arg–Ura supplemented with L-canavanine and G418 or SC/MSG –His–Arg supplemented with L-canavanine, G418 and clonNAT, to select for *MAT***a** double-mutant meiotic progeny. *MAT***a** double-mutant progeny with growth defects were identified by scoring colony area as compared to that of progeny derived from wild-type control screens. Synthetic sick or synthetic lethal interactions were confirmed by tetrad dissection or random spore analysis.

For random spore analysis, spores were inoculated in 3 ml of liquid haploid selection medium (SC medium lacking histidine and arginine but containing canavanine; SC –His –Arg +canavanine) and incubated at 30 °C for 2 d. The germinated *MAT***a** spore progeny were diluted in sterile distilled, deionized water and plated out on medium that selects for the query-gene mutation (SC/MSG –His–Arg +canavanine/clonNAT), the deletion mutant array (DMA) mutation (SC/MSG –His–Arg +canavanine/G418) or both the query-gene and DMA mutations (SC/MSG –His–Arg +canavanine/clonNAT/G418), then incubated at 30 °C for ~2 d. Colony growth under the three conditions was compared and the double mutants were scored as synthetic sick (SS), synthetic lethal (SL) or no interaction (No).

Alternatively, spores were resuspended in sterile distilled, deionized water and plated out on the haploid selection medium (SC –His–Arg +canavanine) and medium selecting for the query-gene mutation, the DMA mutation and both the query-gene and DMA mutations, then incubated at 30 °C for ~2 d. Colony growth under the four conditions was compared and double mutants were scored as synthetic sick (SS), synthetic lethal (SL) or no interaction (No).

Data analysis and visualization. Colony size on yeast array plates was determined using an automated scoring system (H.D., A.Y.H. Tong, M.D. Robinson, H. Xu and C.B., unpublished data). Colony area was measured from digital images of the plates. For the purpose of computer-based scoring, the values of *t* statistics and *P* values were calculated by comparing colony growth on drug medium to that on no-drug control medium. Clustering was executed using MATLAB (Mathworks) and standard hierarchical agglomerative clustering of a binary matrix (a matrix of 1s and 0s). Interaction maps were created using the network visualization system Osprey[39]. The probability of overlap by chance between chemical-genetic and genetic profiles was estimated by

$$P = \frac{P(N_{SGA}, N_{hit})}{P(N, N_{hit})} \frac{P(N_{drug}, N_{hit})}{P(N, N_{hit})}$$

where N_{SGA} is the number of genetic interactions, N_{drug} is the number of chemical-genetic interactions, N_{hit} is the number of overlapping interactions and N is the number of interactions tested (the number of strains in the array) and $P(N,M) = N!/(M!(N - M)!)$. A defined subset of Gene Ontology (GO) functional annotations[40] relevant to the pathways highlighted in this study was used to annotate each gene in the genetic interaction dataset for color coding in network diagrams (see **Supplementary Table 5** online). Genes not falling into any of these categories were designated as 'other'. For genes assigned multiple functional annotations, we chose one that we considered the most probable on the basis of a review of published abstracts for studies concerning the gene. References for all genes in this study can be found at the Saccharomyces Genome Database (SGD; (www.yeastgenome.org), the Yeast Proteome Database (YPD; www.proteome.com) and the Comprehensive Yeast Genome Database (CYGD) at MIPS (http://mips.gsf.de/)[41]. All genetic interaction data is available at the General Repository for Interaction Datasets (GRID; http://biodata.mshri.on.ca/grid)[42].

Note: Supplementary information is available on the Nature Biotechnology website.

ACKNOWLEDGMENTS

We thank D. Drubin for *tub2-403* and M. Cyert, J. Anderson and S. Brill for gifts of FK506, fluconazole and camptothecin, respectively. We thank H. Lu, X. Xin and V. Ghandi for assistance with drug screening and confirmations and Y. Chen and X. Cheng for assistance with SGA screening. This work was supported by grants from the Canadian Institute of Health Research (CIHR) to C.B. and T.R.H. and from the National Cancer Institute of Canada (NCIC) to G.W.B. A.B.P holds a Natural Sciences and Engineering Research Council of Canada (NSERC) graduate student fellowship.

COMPETING INTERESTS STATEMENT

The authors declare that they have no competing financial interests.

Received 25 September; accepted 29 October 2003
Published online at http://www.naturebiotechnology.com/

1. Winzeler, E.A. *et al.* Functional characterization of the *S. cerevisiae* genome by gene deletion and parallel analysis. *Science* **285**, 901–906 (1999).
2. Hughes, T.R. *et al.* Functional discovery via a compendium of expression profiles. *Cell* **102**, 109–926 (2000).
3. Marton, M.J. *et al.* Drug target validation and identification of secondary drug target effects using DNA microarrays. *Nat. Med.* **4**, 1293–1301 (1998).
4. Hartwell, L.H., Szankasi, P., Roberts, C.J., Murray, A.W. & Friend, S.H. Integrating genetic approaches into the discovery of anticancer drugs. *Science* **278**, 1064–1068 (1997).

5. Tong, A.H. *et al.* Systematic genetic analysis with ordered arrays of yeast deletion mutants. *Science* **294**, 2364–2368 (2001).
6. Thomas, J.H., Neff, N.F. & Botstein, D. Isolation and characterization of mutations in the β-tubulin gene of *Saccharomyces cerevisiae*. *Genetics* **111**, 715–734 (1985).
7. Liu, J. *et al.* Calcineurin is a common target of cyclophilin-cyclosporin A and FKBP-FK506 complexes. *Cell* **66**, 807–815 (1991).
8. Rittberg, D.A. & Wright, J.A. Relationships between sensitivity to hydroxyurea and 4-methyl-5-amino-1-formylisoquinoline thiosemicarbazone (MAIO) and ribonucleotide reductase RNR2 mRNA levels in strains of *Saccharomyces cerevisiae*. *Biochem. Cell. Biol.* **67**, 352–357 (1989).
9. Hsiang, Y.H., Lihou, M.G. & Liu, L.F. Arrest of replication forks by drug-stabilized topoisomerase I–DNA cleavable complexes as a mechanism of cell killing by camptothecin. *Cancer Res.* **49**, 5077–5082 (1989).
10. Turi, T.G. & Loper, J.C. Multiple regulatory elements control expression of the gene encoding the *Saccharomyces cerevisiae* cytochrome P450, lanosterol 14 α-demethylase (ERG11). *J. Biol. Chem.* **267**, 2046–2056 (1992).
11. Truan, G., Epinat, J.C., Rougeulle, C., Cullin, C. & Pompon, D. Cloning and characterization of a yeast cytochrome b5-encoding gene which suppresses ketoconazole hypersensitivity in a NADPH-P-450 reductase-deficient strain. *Gene* **142**, 123–127 (1994).
12. Zheng, X.F., Florentino, D., Chen, J., Crabtree, G.R. & Schreiber, S.L. TOR kinase domains are required for two distinct functions, only one of which is inhibited by rapamycin. *Cell* **82**, 121–130 (1995).
13. Kuo, S.C. & Lampen, J.O. Tunicamycin—an inhibitor of yeast glycoprotein synthesis. *Biochem. Biophys. Res. Commun.* **58**, 287–295 (1974).
14. Cutler, N.S., Heitman, J. & Cardenas, M.E. STT4 is an essential phosphatidylinositol 4-kinase that is a target of wortmannin in *Saccharomyces cerevisiae*. *J. Biol. Chem.* **272**, 27671–27677 (1997).
15. Falco, S.C. & Dumas, K.S. Genetic analysis of mutants of *Saccharomyces cerevisiae* resistant to the herbicide sulfometuron methyl. *Genetics* **109**, 21–35 (1985).
16. Parsons, W.J., Ramkumar, V. & Stiles, G.L. Isobutylmethylxanthine stimulates adenylate cyclase by blocking the inhibitory regulatory protein, Gi. *Mol. Pharmacol.* **34**, 37–41 (1988).
17. Garrett-Engele, P., Moilanen, B. & Cyert, M.S. Calcineurin, the Ca^{2+}/calmodulin-dependent protein phosphatase, is essential in yeast mutants with cell integrity defects and in mutants that lack a functional vacuolar H^+-ATPase. *Mol. Cell. Biol.* **15**, 4103–4114 (1995).
18. Bauer, B.E., Wolfger, H. & Kuchler, K. Inventory and function of yeast ABC proteins: about sex, stress, pleiotropic drug and heavy metal resistance. *Biochim. Biophys. Acta* **1461**, 217–236 (1999).
19. Mukhopadhyay, K., Kohli, A. & Prasad, R. Drug susceptibilities of yeast cells are affected by membrane lipid composition. *Antimicrob. Agents Chemother.* **46**, 3695–3705 (2002).
20. Yoshida, S. & Anraku, Y. Characterization of staurosporine-sensitive mutants of *Saccharomyces cerevisiae*: vacuolar functions affect staurosporine sensitivity. *Mol. Gen. Genet.* **263**, 877–888 (2000).
21. Simon, S., Roy, D. & Schindler, M. Intracellular pH and the control of multidrug resistance. *Proc. Natl. Acad. Sci. USA* **91**, 1128–1132 (1994).
22. Ma, L. & Center, M.S. The gene encoding vacuolar H^+-ATPase subunit C is overexpressed in multidrug-resistant HL60 cells. *Biochem. Biophys. Res. Commun.* **182**, 675–681 (1992).
23. Drose, S. *et al.* Inhibitory effect of modified bafilomycins and concanamycins on P- and V-type adenosine triphosphatases. *Biochemistry* **32**, 3902–3906 (1993).
24. Ouar, Z. *et al.* Inhibitors of vacuolar H^+-ATPase impair the preferential accumulation of daunomycin in lysosomes and reverse the resistance to anthracyclines in drug-resistant renal epithelial cells. *Biochem. J.* **370**, 185–193 (2003).
25. Dohmen, R.J., Wu, P. & Varshavsky, A. Heat-inducible degron: a method for constructing temperature-sensitive mutants. *Science* **263**, 1273–1276 (1994).
26. Cyert, M.S. Genetic analysis of calmodulin and its targets in *Saccharomyces cerevisiae*. *Annu. Rev. Genet.* **35**, 647–672 (2001).
27. Cyert, M.S. & Thorner, J. Regulatory subunit (CNB1 gene product) of yeast Ca^{2+}/calmodulin-dependent phosphoprotein phosphatases is required for adaptation to pheromone. *Mol. Cell. Biol.* **12**, 3460–3469 (1992).
28. Tanida, I., Hasegawa, A., Iida, H., Ohya, Y. & Anraku, Y. Cooperation of calcineurin and vacuolar H^+-ATPase in intracellular Ca^{2+} homeostasis of yeast cells. *J. Biol. Chem.* **270**, 10113–10119 (1995).
29. Aasland, R., Stewart, A.F. & Gibson, T. The SANT domain: a putative DNA-binding domain in the SWI-SNF and ADA complexes, the transcriptional co-repressor N-CoR and TFIIIB. *Trends Biochem. Sci.* **21**, 87–88 (1996).
30. Boyer, L.A. *et al.* Essential role for the SANT domain in the functioning of multiple chromatin remodeling enzymes. *Mol. Cell.* **10**, 935–942 (2002).
31. Bellaoui, M. *et al.* Elg1 forms an alternative RFC complex important for DNA replication and genome integrity. *EMBO J.* **22**, 4304–13 (2003).
32. Ben-Aroya, S., Koren, A., Liefshitz, B., Steinlauf, R. & Kupiec, M. ELG1, a yeast gene required for genome stability, forms a complex related to replication factor C. *Proc. Natl. Acad. Sci. USA* **100**, 9906–9911 (2003).
33. Ersfeld, K. *et al.* Characterization of the tubulin-tyrosine ligase. *J. Cell. Biol.* **120**, 725–732 (1993).
34. Shoemaker, D.D., Lashkari, D.A., Morris, D., Mittmann, M. & Davis, R.W. Quantitative phenotypic analysis of yeast deletion mutants using a highly parallel molecular barcoding strategy. *Nat. Genet.* **14**, 450–456 (1996).
35. Giaever, G. *et al.* Genomic profiling of drug sensitivities via induced haploinsufficiency. *Nat. Genet.* **21**, 278–283 (1999).
36. Barstead, R. Genome-wide RNAi. *Curr. Opin. Chem. Biol.* **5**, 63–66 (2001).
37. Shi, Y. Mammalian RNAi for the masses. *Trends Genet.* **19**, 9–12 (2003).
38. Brachmann, C.B. *et al.* Designer deletion strains derived from *Saccharomyces cerevisiae* S288C: a useful set of strains and plasmids for PCR-mediated gene disruption and other applications. *Yeast* **14**, 115–132 (1998).
39. Breitkreutz, B.J., Stark, C. & Tyers, M. Osprey: a network visualization system. *Genome Biol.* **4**, R22 (2003).
40. Ashburner, M. *et al.* Gene ontology: tool for the unification of biology. The Gene Ontology Consortium. *Nat. Genet.* **25**, 25–29 (2000).
41. Mewes, H.W., Albermann, K., Heumann, K., Liebl, S. & Pfeiffer, F. MIPS: a database for protein sequences, homology data and yeast genome information. *Nucleic Acids Res.* **25**, 28–30 (1997).
42. Breitkreutz, B.J., Stark, C. & Tyers, M. The GRID: the General Repository for Interaction Datasets. *Genome Biol.* **4**, R23 (2003).